Generic Long-Range Interactions Between Passive Bodies in an Active Fluid

Generic Long-Range Interactions Between Passive Bodies in an Active Fluid

Yongjoo Baek,[1,2,*] Alexandre P. Solon,[3] Xinpeng Xu,[1,4] Nikolai Nikola,[1] and Yariv Kafri[1]
[1]Department of Physics, Technion—Israel Institute of Technology, Haifa 32000, Israel
[2]DAMTP, Centre for Mathematical Sciences, University of Cambridge, Cambridge CB3 0WA, United Kingdom
[3]Department of Physics, Massachusetts Institute of Technology, Cambridge, Massachusetts 02139, USA
[4]Department of Physics, Guangdong Technion—Israel Institute of Technology, Shantou, Guangdong 515063, People's Republic of China

(Received 19 September 2017; published 31 January 2018)

A single nonspherical body placed in an active fluid generates currents via breaking of time-reversal symmetry. We show that, when two or more passive bodies are placed in an active fluid, these currents lead to long-range interactions. Using a multipole expansion, we characterize their leading-order behaviors in terms of single-body properties and show that they decay as a power law with the distance between the bodies, are anisotropic, and do not obey an action-reaction principle. The interactions lead to rich dynamics of the bodies, illustrated by the spontaneous synchronized rotation of pinned nonchiral bodies and the formation of traveling bound pairs. The occurrence of these phenomena depends on tunable properties of the bodies, thus opening new possibilities for self-assembly mediated by active fluids.

DOI: 10.1103/PhysRevLett.120.058002

Active matter is a class of nonequilibrium systems in which energy is converted into systematic motion on a microscopic scale [1]. They have attracted much attention [2,3] due to a host of interesting physical phenomena [4–9], their relevance to many biological systems [10–13], and their potential use for self-assembly applications [14]. They have also been suggested as tools for novel engineering applications—for example, active fluids have been used to power microscopic gears [15–21]. This results from the fact that, when an asymmetric body is immersed in a fluid with broken time-reversal symmetry, it experiences a net force [22–24] that is coupled to the generation of ratchetlike currents [25,26].

In this Letter, we study passive bodies immersed in an active fluid. We show that the ratchetlike currents generated by each body give rise to forces and torques that decay as a power law with distance, are anisotropic, and do not obey an action-reaction principle. Using a multipole expansion, the leading-order behavior of the interactions can be expressed in terms of single-body quantities that can be measured independently in experiments or numerical simulations. Moreover, by designing the two bodies, one can control the amplitude and polarity of the interactions between them. This leads to a host of interesting dynamical phenomena of which we illustrate two: the spontaneous synchronized rotations of pinned rotors and the formation of traveling bound pairs. Our results suggest a new method for self-assembly by embedding passive bodies in an active fluid.

We stress that the interactions studied here exist even between nonmoving bodies and are therefore distinct from usual hydrodynamic interactions [27]. They are also different from thermal Casimir interactions [28,29], because they do not rely on correlations between the fluid particles and are present even in a dilute active fluid. Finally, we note that previous studies [30–32] have numerically observed interactions induced by confinement that exponentially decay over a characteristic length scale. Although the decay length can be large (much greater than the size of an active particle), these interactions have a finite range and are thus qualitatively different from our results, which show scale-free interactions, decaying as a power law.

Model.—We base our study on a common model of an active fluid consisting of N pointlike particles, which do not interact among themselves and self-propel at a constant speed v in two dimensions. The position $\mathbf{r}_i$ and the orientation θ_i of active particle i evolve according to the overdamped Langevin equations

$$\dot{\mathbf{r}}_i = v\mathbf{e}_{\theta_i} - \mu\sum_j \boldsymbol{\nabla} V_j + \sqrt{2D_t}\boldsymbol{\eta}_i, \qquad \dot{\theta}_i = \sqrt{2D_r}\xi_i. \quad (1)$$

Here $\mathbf{e}_{\theta_i} \equiv (\cos\theta_i, \sin\theta_i)$ is the heading of particle i, μ is its mobility, D_t and D_r are translational and rotational diffusivities, and $\boldsymbol{\eta}_i$ and ξ_i are Gaussian white noises of unit variance. The presence of body j in the active fluid is described by a potential V_j describing the interaction between each active particle and the passive body j. The dots denote derivatives with respect to time. In addition, we allow the particles to randomize their orientation at a constant tumbling rate α. This dynamics encompass the two well-studied models of run-and-tumble particles (with $\alpha \neq 0$ and $D_r = 0$) [33] and active Brownian particles (having $\alpha = 0$ and $D_r \neq 0$) [34,35]. There has been much recent progress [24,26,36–49] in the characterization of

forces in this class of systems and we build upon it. Note that the model falls into the class of dry active systems, which do not conserve momentum. As such, it is best suited for describing the dynamics of particles next to a surface, for example, those of vibrated granular monolayers [50–52] or gliding bacteria [53].

A single passive body.—We first discuss the effects of a single passive body on an active fluid. For future reference, we maintain the index j, although, in this case, body j is the only passive body in the system. Using standard methods [54,55] (also detailed in [56]), Eq. (1) leads to an exact equation for the active particle density ρ_j (j marking the dependence on V_j) in the steady state

$$D_{\text{eff}}\nabla^2\rho_j = -\mu\boldsymbol{\nabla}\cdot(\rho_j\boldsymbol{\nabla}V_j) + \sum_{a,b}\partial_a\partial_b(\mathbb{G}_j)_{ab}. \quad (2)$$

Here $D_{\text{eff}} \equiv D_t + vl_r/2$ is the effective diffusion constant of the active particles, $l_r \equiv v/(\alpha + D_r)$ is their run length, indices a and b run over the Cartesian coordinates $\{x, y\}$, and $\mathbb{G}_j$ is a rank 2 tensor containing information about active particle orientations. In the far-field limit (at distances r much larger than the diameter of the body and the run length l_r), the solution of Eq. (2) can be written to dipole order in a multipole expansion as

$$\rho_j(\mathbf{r}) = \rho_b + \frac{\beta_{\text{eff}}}{2\pi}\frac{\mathbf{r}\cdot\mathbf{p}_j}{r^2} + O(r^{-2}), \quad (3)$$

where ρ_b denotes the bulk density of active particles and $\beta_{\text{eff}} \equiv \mu/D_{\text{eff}}$ is their effective inverse temperature. The dipole moment $\mathbf{p}_j$, obtained as

$$\mathbf{p}_j = -\int d^2\mathbf{r}'\rho_j\boldsymbol{\nabla}'V_j, \quad (4)$$

is equal to the total force exerted by body j on the active particles. Alternatively, $-\mathbf{p}_j$ is the propulsion force applied by the active particles on body j. We stress that, at this order, Eqs. (3) and (4) are exact, with $\mathbb{G}_j$ in Eq. (2) only contributing to higher-order multipoles in the far field. While $\mathbf{p}_j$ is easily measurable from Eq. (4), its first-principle calculation is difficult due to complex near-field effects of $\mathbb{G}_j$. However, as shown in [56], it can be perturbatively obtained for shallow potentials $\beta_{\text{eff}}|\nabla V_j| \ll 1$, explicitly confirming that asymmetric V_j induces $\mathbf{p}_j \neq \mathbf{0}$.

The associated far-field current density is dominated by the diffusive component

$$\mathbf{J}_j(\mathbf{r}) \simeq -D_{\text{eff}}\boldsymbol{\nabla}\rho_j \simeq -\frac{\mu}{2\pi}\left(\frac{\mathbf{p}_j}{r^2} - \frac{2(\mathbf{r}\cdot\mathbf{p}_j)\mathbf{r}}{r^4}\right), \quad (5)$$

which resembles the electric field of a charge dipole. The forms of ρ_j and $\mathbf{J}_j$ are equivalent to those of the density and current fields generated by a local pump applying a point force $\mathbf{p}_j$ on a passive diffusive medium [57]. In this sense, an asymmetric passive body in an active fluid acts like a pump, although its power is supplied not by an external source, but by the active particles themselves.

Forces between passive bodies.—We now consider two passive bodies described by potentials V_1 and V_2, with dipole moments (in isolation) $\mathbf{p}_1$ and $\mathbf{p}_2$, and position vectors $\mathbf{R}_1$ and $\mathbf{R}_2$. We set $\mathbf{R}_2 = \mathbf{0}$ and $\mathbf{R}_1 = \mathbf{r}_{12}$ and work in the far-field limit where $r_{12} = |\mathbf{r}_{12}|$ is much larger than the run length l_r and the diameters of the bodies. Denoting by ρ the steady-state density field of active particles, the force applied by the active particles on body j is given by $\int d^2\mathbf{r}\rho\boldsymbol{\nabla}V_j$, with $j \in \{1, 2\}$. We define the force applied by body 1 on body 2 as $\mathbf{F}_{12} = \mathbf{p}_2 + \int d^2\mathbf{r}\rho\boldsymbol{\nabla}V_2$, which is the change in the force acting on body 2 due to the presence of body 1 [recall that $-\mathbf{p}_2$, given by Eq. (4), is the force acting on isolated body 2]. This stems from the change of ρ near body 2 induced by body 1, which can be expressed as a series expansion in r_{12}^{-1} (see [56] for a detailed derivation). It is convenient to separate the total force into two components $\mathbf{F}_{12} = \mathbf{F}^a_{12} + \mathbf{F}^s_{12}$, where $\mathbf{F}^a_{12}$ acts only on asymmetric bodies with nonzero $\mathbf{p}_j$, while $\mathbf{F}^s_{12}$ is present even for symmetric bodies with $\mathbf{p}_j = 0$. Then we find

$$\mathbf{F}^a_{12} = -\frac{\beta_{\text{eff}}}{2\pi\rho_b}\frac{\mathbf{r}_{12}\cdot\mathbf{p}_1}{r_{12}^2}\mathbf{p}_2 + O(r_{12}^{-2}), \quad (6)$$

$$\mathbf{F}^s_{12} = \frac{\mathbb{R}_2\mathbf{J}_1(\mathbf{r}_{12})}{\rho_b} + O(r_{12}^{-3}). \quad (7)$$

Here $\mathbb{R}_2$ is the inverse mobility tensor of body 2 due to the active particles. It is measured by placing body 2 alone in an active fluid of average density ρ_b, through which a boundary-driven diffusive current $\rho_b\mathbf{u}$ is flowing. Then $\mathbb{R}_2$ is calculated from

$$(\mathbb{R}_2)_{ab} = \frac{\partial}{\partial u_b}\left[\mathbf{F}_2^{(\mathbf{u})}\cdot\mathbf{e}_a\right]\Big|_{\mathbf{u}=\mathbf{0}}, \quad (8)$$

where indices a and b stand for Cartesian coordinates $\{x, y\}$, $\mathbf{e}_a$ is a unit vector in the a direction, and $\mathbf{F}_2^{(\mathbf{u})}$ is the steady-state force on the body. Finally, $\mathbf{J}_1$ in Eq. (7) is given by Eq. (5). At this order, the interactions between the two bodies are thus completely determined by $\mathbf{p}_1$, $\mathbf{p}_2$, and $\mathbb{R}_2$, which are single-body quantities that can be measured independently.

We can understand Eqs. (6) and (7) intuitively in terms of the density and current fields produced by body 1 alone. First, we note that body 2 experiences a propulsion force $-\mathbf{p}_2$ in the absence of body 1. Because of the mutual independence of active particles, the propulsion force is proportional to the bulk density ρ_b. With body 1 added, its dipole density field changes the effective bulk density felt by body 2 from ρ_b to $\rho_1(\mathbf{r}_{12})$, given in Eq. (3). This leads to

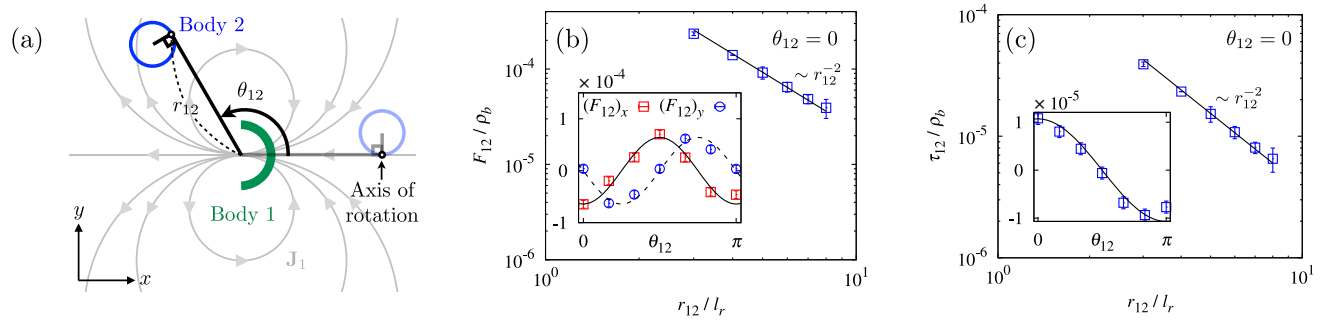

FIG. 1. Dipole contributions to far-field interactions. (a) The numerical setup used to verify the theoretical predictions. A circular body is placed at different distances r_{12} and angles θ_{12} away from a semicircular body that generates a dipole current. (b) The force normalized by the bulk density as a function of r_{12}/l_r, with l_r the run length, for $\theta_{12} = 0$. (Inset) The dependence of the force components $(F_{12})_{x,y}$ in the x and y directions as a function of θ_{12}. (c) The torque applied by the semicircle on a circle that is held tangent to $\mathbf{r}_{12}$ and pinned at the contact point as θ_{12} is varied; see (a). The lines in (b) and (c) correspond to the theory with no fitting parameters. All the parameters and units of the simulations are specified in the Supplemental Material [56].

Eq. (6), with $\mathbf{F}_{12}^a \sim r_{12}^{-1}$. Therefore, $\mathbf{F}_{12}^a$ only induces a correction to the speed of the body.

Meanwhile, $\mathbf{F}_{12}^s \sim r_{12}^{-2}$ stems from the force on body 2 due to the current field $\mathbf{J}_1(\mathbf{r}_{12}) \sim r_{12}^{-2}$ generated by body 1 in accordance with Eq. (5). At large r_{12}, the induced force can be linearized as $\mathbb{R}_2\mathbf{J}_1(\mathbf{r}_{12})/\rho_b$. Note that $\mathbf{F}_{12}^s$ can change the propulsion direction of body 2. In Fig. 1, we present a measurement of the force $\mathbf{F}_{12}$ on a circular body (so that $\mathbf{p}_2 = \mathbf{0}$). In this case, $\mathbb{R}_2$ is proportional to the identity matrix and we evaluated it numerically. The results agree nicely with the theory using no fitting parameters, although on a reduced range because of numerical limitations.

Torques between passive bodies.—The torque $\boldsymbol{\tau}_{12}$ exerted by body 1 on body 2 can be obtained using the same approach. We denote by $\boldsymbol{\tau}_j = \int d^2\mathbf{r}'\rho_j(\mathbf{r}')(\mathbf{r}' - \mathbf{R}_j) \times \boldsymbol{\nabla}' V_j$ the self-torque on an isolated body j with respect to the reference position $\mathbf{R}_j$. It is useful to decompose the result into a correction to the self-torque $\boldsymbol{\tau}_{12}^a$, which is dominant when $\boldsymbol{\tau}_2 \neq \mathbf{0}$, and a subleading contribution $\boldsymbol{\tau}_{12}^s$, which induces a torque even when $\boldsymbol{\tau}_2 = \mathbf{0}$. We find

$$\boldsymbol{\tau}_{12}^a = \frac{\beta_{\mathrm{eff}}}{2\pi\rho_b}\frac{\mathbf{r}_{12}\cdot\mathbf{p}_1}{r_{12}^2}\boldsymbol{\tau}_2 + O(r_{12}^{-2}), \tag{9}$$

$$\boldsymbol{\tau}_{12}^s = \frac{\boldsymbol{\gamma}_2}{\rho_b} \times \mathbf{J}_1(\mathbf{r}_{12}) + O(r_{12}^{-3}), \tag{10}$$

where the vector $\boldsymbol{\gamma}_2$, similar to $\mathbb{R}_2$, characterizes the response of isolated body 2 to a diffusive current $\rho_b\mathbf{u}$ carried by an active fluid of mean density ρ_b. The vector is calculated from the steady-state torque $\boldsymbol{\tau}_2^{(\mathbf{u})}$ exerted on body 2 according to

$$\boldsymbol{\gamma}_2 = \left[\boldsymbol{\nabla}_{\mathbf{u}} \times \boldsymbol{\tau}_2^{(\mathbf{u})}\right]\Big|_{\mathbf{u}=\mathbf{0}}. \tag{11}$$

As with Eqs. (6) and (7), $\boldsymbol{\tau}_{12}^a$ results from a local shift in the density and $\boldsymbol{\tau}_{12}^s$ from the current. The latter tends to align $\boldsymbol{\gamma}_2$ with the current. In Fig. 1, our predictions are compared with simulations that measure the torque exerted by a semicircle (body 1) on a circle (body 2) held at its edge, with $\boldsymbol{\gamma}_2$ evaluated numerically.

A few comments on the properties of the interactions are in order. First, even in the presence of three or more passive bodies, at large mutual distances, the interactions are still dominated by pairwise components. Second, going one order higher in the multipole expansion, one finds that two rodlike bodies interact through quadrupole moments. Previous studies [30–32] on the same setup focused on the near-field effects that decay exponentially with distance, but we predict this interaction to be much longer ranged, decaying as r_{12}^{-3}. Numerical support is provided in [56]. Finally, an extension of the analysis to dimensions $d > 2$ yields $\mathbf{F}_{12}^a \sim r_{12}^{-(d-1)}$ and $\mathbf{F}_{12}^s \sim r_{12}^{-d}$, with corresponding changes to the torques.

We note that the interactions discussed above are anisotropic and do not satisfy the action-reaction principle. For passive bodies allowed to move in the active fluid, these features lead to a host of interesting dynamical phenomena. Assuming overdamped bodies, we take

$$\begin{aligned}\dot{\mathbf{R}}_j &= \mu_j^T \int d^2\mathbf{r}\rho(\mathbf{r},t)\boldsymbol{\nabla}V_j,\\ \dot{\Theta}_j &= \mu_j^R \int d^2\mathbf{r}\rho(\mathbf{r},t)[(\mathbf{r}-\mathbf{R}_j)\times\boldsymbol{\nabla}V_j]\cdot\mathbf{e}_z,\end{aligned} \tag{12}$$

where μ_j^T and μ_j^R are the translational and rotational mobilities of body j, Θ_j is an angle giving its orientation with respect to a fixed axis of reference, and $\mathbf{R}_j$ is a position vector. For simplicity, we consider bodies for which the position vector $\mathbf{R}_j$ can be chosen so that no off-diagonal mobilities couple the translational and rotational degrees of freedom. The extension to other cases is straightforward. The results derived above are applicable when the mobilities are small enough so that an adiabatic limit holds: at

each instant, the system can be considered to be in a steady state with fixed bodies. We do not specify direct (short-range) interactions between the bodies, since here we consider only far-field effects. Interestingly, we show that properties of the bodies can be tuned to lead to distinct phenomena.

For concreteness, we consider pairs of semicircles. A semicircle traps active particles approaching from the concave side ("rear"), while those on the convex side ("front") easily slide past the body. This creates a backward current of active particles, associated with an opposing force [26], which propels the semicircle forward [see Fig. 1(a)]. In the terminology introduced above, a semicircle has a nonzero dipole moment $\mathbf{p}_j$ pointing in the backward direction. We focus on two types of semicircles that rotate around $\mathbf{R}_j$ either at the apex (type A) or at the center of the circle (type C). In experiments, this could be achieved by properly designing the bodies. Most importantly, for their dynamics, $\boldsymbol{\gamma}_j$ is parallel to $\mathbf{p}_j$ for type C bodies and antiparallel for type A bodies. In both cases, $\mathbf{R}_j$ is on the symmetry axis so that $\boldsymbol{\tau}_A = \boldsymbol{\tau}_C = \mathbf{0}$.

Spontaneous synchronized rotations of pinned rotors.—We consider a pair of semicircles, one type A, pinned to the surface at its apex, and one type C, pinned to the surface at its center. They are placed at a distance much larger than l_r so that we can understand their dynamics in terms of the far-field torques given in Eq. (10). The torques align $\boldsymbol{\gamma}_{A/C}$ with the current generated by the other circle, which depends only on the dipole moment, taken to be equal for both. To describe the dynamics, we define two angles θ_C and θ_A as the orientation of $\boldsymbol{\gamma}_C$ and $\boldsymbol{\gamma}_A$ with respect to the horizontal, as represented in Fig. 2. Note that θ_C is defined with a clockwise convention and θ_A is counterclockwise. Neglecting noise, we can write the dynamics of the angle difference $\theta_C - \theta_A$ in the adiabatic limit as

$$\dot{\theta}_C - \dot{\theta}_A = \frac{1}{\rho_b}(\mu_C^R \boldsymbol{\tau}_{AC} - \mu_A^R \boldsymbol{\tau}_{CA}) \cdot \mathbf{e}_z = -\frac{\mu_A^R J_A \gamma_C - \mu_C^R J_C \gamma_A}{\rho_b} \sin(\theta_C - \theta_A), \tag{13}$$

where $\gamma_j \equiv |\boldsymbol{\gamma}_j|$, $J_j \equiv |\mathbf{J}_j|$. For $\mu_C^R J_A \gamma_C > \mu_A^R J_C \gamma_A$ the angles tend to phase lock at $\theta_C = \theta_A$, while for $\mu_C^R J_A \gamma_C < \mu_A^R J_C \gamma_A$, they phase lock at $\theta_C = \theta_A + \pi$. Using this, we can expand in small deviations from the locking angle difference. The equation for θ_A then reduces to

$$\ddot{\theta}_A = -\frac{1}{\rho_b}|\mu_C^R J_A \gamma_C - \mu_A^R J_C \gamma_A| \dot{\theta}_A. \tag{14}$$

The equation implies that, for general parameters, θ_A is damped and does not rotate persistently along a given direction. However, if $\mu_C^R J_A \gamma_C \simeq \mu_A^R J_C \gamma_A$, the damping is weak and the two rotors persistently counterrotate in a spontaneously chosen direction with the same speed and weak phase-locking interactions. We observe the three types of behavior in simulations as shown in the Supplemental Material Movies SM1–SM3 and Fig. 2(b). On the contrary, it is easily seen that, when both rotors are of the same type, they always phase lock, but do not exhibit persistent rotations. When both are type C (A), the rotors phase lock with an angle difference 0 (π) (see Supplemental Material Movies SM4 and SM5).

Formation of a traveling bound pair.—Here we again consider a type A and type C pair of semicircles. Numerical simulations show that, after a transient regime, the two bodies form a traveling bound pair with type A trailing type C (see Fig. 3(a) and Movie SM6). This behavior can be qualitatively understood in the limit where $\mu_C^R \gg \mu_A^R$. Then the motion of type A is, to leading order, independent of type C, while type C is strongly affected by type A. More precisely, the orientation of the type C body is dictated by

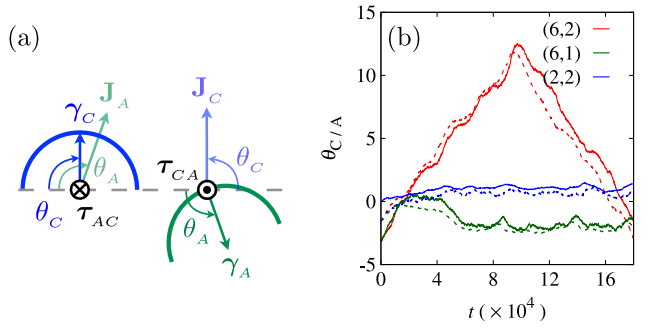

FIG. 2. Phase-locking and spontaneous rotations of pinned rotors. (a) An illustration of type C and type A semicircles pinned to the surface (not shown to scale). In the numerics, the distance between the pinning points of the semicircles is $5l_r$. (b) The history of the angles θ_C (solid lines) and θ_A (dotted lines) for rotational mobilities given by (μ_C^R, μ_A^R). In case (2,2), the solid line indicates $\theta_C + \pi$ instead of θ_C. All the parameters and units of the simulations are specified in the Supplemental Material [56].

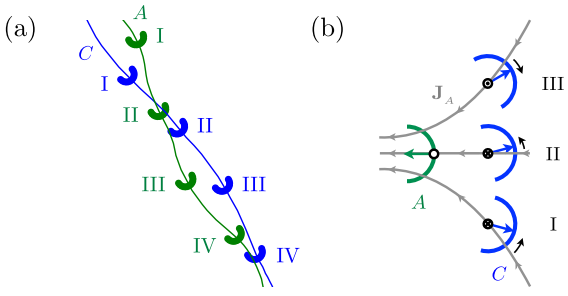

FIG. 3. (a) A stroboscopic image of a traveling bound pair obtained from the numerics, with consecutive positions marked by I–IV. All the parameters and units of the simulations are specified in the Supplemental Material [56]. (b) A schematic illustration of the torques experienced by a type C body in the current field of a type A body. I, II, and III indicate consecutive relative positions during the snakelike motion. Note that the torque directions are consistent with the resulting motion.

its tendency to align γ_C with $\mathbf{J}_A$. This leads to a snakelike motion in front of the type A body explained graphically in Fig. 3(b). Other pairings of semicircles lead to different phenomena, including antialignment and the formation of bound pairs, although in this last case, the effect depends on near-field interactions. These are expected to be less universal than the far-field interactions and we reserve their study for future work.

In summary, we have explored the long-range interactions occurring generically between passive bodies placed in an active fluid. We have shown that, at first order in a multipole expansion, an asymmetric body generates dipolar currents which decay algebraically in space. These mediate generic long-range forces and torques between passive bodies, which can be expressed in terms of a few single-body quantities. Interestingly, the interactions can be tuned by designing the shape of the bodies, which may provide new routes for designing self-assembling materials. We gave two examples of dynamical phenomena induced by the far-field interactions. Considering also near-field effects should reveal many more. Finally, we note that the physics described relies only on the breaking of time-reversal symmetry and a diffusive behavior at large length scale. Therefore, it should be generically present in a broad range of active systems, even including those with mutual interactions between active particles. It would be interesting to check this explicitly using several recent theoretical frameworks [58–60], which have been proposed as approximate descriptions of systems with interacting active particles. Possible relevance of these effects to flocking transitions in shaken granular systems [61] is also of interest.

Y. B., N. N., and Y. K. are supported by an I-CORE Program of the Planning and Budgeting Committee of the Israel Science Foundation and an Israel Science Foundation grant. Y. B. received partial support at the Technion from a Lady Davis Foundation Fellowship. A. P. S. is supported by the Gordon and Betty Moore Foundation through a PLS Fellowship. X. X. is supported by Guangdong-Technion Postdoctoral Fellowship.

*y.baek@damtp.cam.ac.uk

[1] S. Ramaswamy, Annu. Rev. Condens. Matter Phys. **1**, 323 (2010).
[2] M. C. Marchetti, J. F. Joanny, S. Ramaswamy, T. B. Liverpool, J. Prost, M. Rao, and R. A. Simha, Rev. Mod. Phys. **85**, 1143 (2013).
[3] C. Bechinger, R. Di Leonardo, H. Löwen, C. Reichhardt, G. Volpe, and G. Volpe, Rev. Mod. Phys. **88**, 045006 (2016).
[4] T. Vicsek, A. Czirók, E. Ben-Jacob, I. Cohen, and O. Shochet, Phys. Rev. Lett. **75**, 1226 (1995).
[5] T. Vicsek and A. Zafeiris, Phys. Rep. **517**, 71 (2012).
[6] J. Toner, Y. Tu, and S. Ramaswamy, Ann. Phys. (Amsterdam) **318**, 170 (2005).
[7] M. E. Cates and J. Tailleur, Annu. Rev. Condens. Matter Phys. **6**, 219 (2015).
[8] S. Henkes, Y. Fily, and M. C. Marchetti, Phys. Rev. E **84**, 040301 (2011).
[9] M. Sheinman, A. Sharma, J. Alvarado, G. H. Koenderink, and F. C. MacKintosh, Phys. Rev. Lett. **114**, 098104 (2015).
[10] D. Chowdhury, A. Schadschneider, and K. Nishinari, Phys. Life Rev. **2**, 318 (2005).
[11] A. B. Kolomeisky and M. E. Fisher, Annu. Rev. Phys. Chem. **58**, 675 (2007).
[12] F. Jülicher, K. Kruse, J. Prost, and J. Joanny, Phys. Rep. **449**, 3 (2007).
[13] D. Chowdhury, Phys. Rep. **529**, 1 (2013).
[14] R. Soto and R. Golestanian, Phys. Rev. Lett. **112**, 068301 (2014); Phys. Rev. E **91**, 052304 (2015).
[15] L. Angelani and R. Di Leonardo, New J. Phys. **12**, 113017 (2010).
[16] A. Kaiser, A. Peshkov, A. Sokolov, B. ten Hagen, H. Löwen, and I. S. Aranson, Phys. Rev. Lett. **112**, 158101 (2014).
[17] A. Kaiser, A. Sokolov, I. S. Aranson, and H. Löwen, Eur. Phys. J. Spec. Top. **224**, 1275 (2015).
[18] L. Angelani, R. Di Leonardo, and G. Ruocco, Phys. Rev. Lett. **102**, 048104 (2009).
[19] A. Sokolov, M. M. Apodaca, B. A. Grzybowski, and I. S. Aranson, Proc. Natl. Acad. Sci. U.S.A. **107**, 969 (2010).
[20] R. Di Leonardo, L. Angelani, D. Dell'Arciprete, G. Ruocco, V. Iebba, S. Schippa, M. P. Conte, F. Mecarini, F. De Angelis, and E. Di Fabrizio, Proc. Natl. Acad. Sci. U.S.A. **107**, 9541 (2010).
[21] H. Li and H. P. Zhang, Europhys. Lett. **102**, 50007 (2013).
[22] C. J. O. Reichhardt and C. Reichhardt, Annu. Rev. Condens. Matter Phys. **8**, 51 (2017).
[23] S. A. Mallory, C. Valeriani, and A. Cacciuto, Phys. Rev. E **90**, 032309 (2014).
[24] W. Yan and J. F. Brady, J. Fluid Mech. **785** (2015).
[25] J. Tailleur and M. E. Cates, Europhys. Lett. **86**, 60002 (2009).
[26] N. Nikola, A. P. Solon, Y. Kafri, M. Kardar, J. Tailleur, and R. Voituriez, Phys. Rev. Lett. **117**, 098001 (2016).
[27] J. Happel and H. Brenner, *Low Reynolds Number Hydrodynamics: With Special Applications to Particulate Media* (Martinuis Nijhoff, The Hague, 1983).
[28] M. E. Fisher and P.-G. de Gennes, C. R. Acad. Sci. (Paris) Ser. B **287**, 207 (1978).
[29] M. Kardar and R. Golestanian, Rev. Mod. Phys. **71**, 1233 (1999).
[30] D. Ray, C. Reichhardt, and C. J. O. Reichhardt, Phys. Rev. E **90**, 013019 (2014).
[31] J. Harder, S. A. Mallory, C. Tung, C. Valeriani, and A. Cacciuto, J. Chem. Phys. **141**, 194901 (2014).
[32] R. Ni, M. A. Cohen Stuart, and P. G. Bolhuis, Phys. Rev. Lett. **114**, 018302 (2015).
[33] M. J. Schnitzer, Phys. Rev. E **48**, 2553 (1993).
[34] F. Schweitzer, W. Ebeling, and B. Tilch, Phys. Rev. Lett. **80**, 5044 (1998).
[35] P. Romanczuk, M. Bär, W. Ebeling, B. Lindner, and L. Schimansky-Geier, Eur. Phys. J. Spec. Top. **202**, 1 (2012).
[36] S. A. Mallory, A. Šarić, C. Valeriani, and A. Cacciuto, Phys. Rev. E **89**, 052303 (2014).
[37] X. Yang, M. L. Manning, and M. C. Marchetti, Soft Matter **10**, 6477 (2014).

[38] S. C. Takatori, W. Yan, and J. F. Brady, Phys. Rev. Lett. **113**, 028103 (2014).
[39] Y. Fily, A. Baskaran, and M. F. Hagan, Soft Matter **10**, 5609 (2014).
[40] A. P. Solon, J. Stenhammar, R. Wittkowski, M. Kardar, Y. Kafri, M. E. Cates, and J. Tailleur, Phys. Rev. Lett. **114**, 198301 (2015).
[41] F. Ginot, I. Theurkauff, D. Levis, C. Ybert, L. Bocquet, L. Berthier, and C. Cottin-Bizonne, Phys. Rev. X **5**, 011004 (2015).
[42] S. C. Takatori and J. F. Brady, Phys. Rev. E **91**, 032117 (2015).
[43] W. Yan and J. F. Brady, Soft Matter **11**, 6235 (2015).
[44] A. P. Solon, Y. Fily, A. Baskaran, M. E. Cates, Y. Kafri, M. Kardar, and J. Tailleur, Nat. Phys. **11**, 673 (2015).
[45] R. G. Winkler, A. Wysocki, and G. Gompper, Soft Matter **11**, 6680 (2015).
[46] T. Speck and R. L. Jack, Phys. Rev. E **93**, 062605 (2016).
[47] Y. Fily, Y. Kafri, A. P. Solon, J. Tailleur, and A. Turner, J. Phys. A **51**, 044003 (2018).
[48] C. Sandford and A. Y. Grosberg, Phys. Rev. E **97**, 012602 (2018).
[49] C. Sandford, A. Y. Grosberg, and J.-F. Joanny, Phys. Rev. E **96**, 052605 (2017).
[50] J. Deseigne, O. Dauchot, and H. Chaté, Phys. Rev. Lett. **105**, 098001 (2010).
[51] J. Deseigne, S. Leonard, O. Dauchot, and H. Chaté, Soft Matter **8**, 5629 (2012).
[52] G. Junot, G. Briand, R. Ledesma-Alonso, and O. Dauchot, Phys. Rev. Lett. **119**, 028002 (2017).
[53] F. Peruani, J. Starruß, V. Jakovljevic, L. Søgaard-Andersen, A. Deutsch, and M. Bär, Phys. Rev. Lett. **108**, 098102 (2012).
[54] M. E. Cates and J. Tailleur, Europhys. Lett. **101**, 20010 (2013).
[55] A. P. Solon, M. E. Cates, and J. Tailleur, Eur. Phys. J. Spec. Top. **224**, 1231 (2015).
[56] See Supplemental Material at http://link.aps.org/supplemental/10.1103/PhysRevLett.120.058002 for detailed derivations and simulation methods.
[57] T. Sadhu, S. N. Majumdar, and D. Mukamel, Phys. Rev. E **84**, 051136 (2011).
[58] C. Maggi, U. M. B. Marconi, N. Gnan, and R. Di Leonardo, Sci. Rep. **5**, 10742 (2015).
[59] T. F. F. Farage, P. Krinninger, and J. M. Brader, Phys. Rev. E **91**, 042310 (2015).
[60] É. Fodor, C. Nardini, M. E. Cates, J. Tailleur, P. Visco, and F. van Wijland Phys. Rev. Lett. **117**, 038103 (2016).
[61] N. Kumar, H. Soni, S. Ramaswamy, and A. K. Sood, Nat. Commun. **5**, 5688 (2014).